European Journal of Pharmaceutics and Biopharmaceutics 79 (2011) 197–204

Contents lists available at ScienceDirect

European Journal of Pharmaceutics and Biopharmaceutics

journal homepage: www.elsevier.com/locate/ejpb

Research Paper

Reverse micelle-loaded lipid nanocarriers: A novel drug delivery system for the sustained release of doxorubicin hydrochloride

Sandy Vrignaud [a,b], Nicolas Anton [c,*], Pascal Gayet [a], Jean-Pierre Benoit [a,d], Patrick Saulnier [a]

[a] University of Angers, Inserm U646, Angers, France
[b] Pharmacy, Academic Hospital, Angers, France
[c] University of Strasbourg, Laboratoire de Conception et Application de Molécules Bioactives, équipe de Pharmacie Biogalénique, Illkirch, France
[d] EPHE, Paris, France

ARTICLE INFO

Article history:
Received 14 December 2010
Accepted in revised form 15 February 2011
Available online 21 February 2011

Keywords:
Nanoparticle
Reverse micelle
Low-energy emulsification
Doxorubicin
Docetaxel

ABSTRACT

In this study, we are pioneering new nanotechnology for the encapsulation of anticancer drugs (doxorubicin (DOX) and/or docetaxel (DOCE)), whatever their solubility and water affinity. The purpose of this study is to highlight the potential of this recently patented technology, by carrying out a thorough physicochemical characterisation of these multiscaled nanocarriers, followed by the study of an encapsulation and release model of hydrophilic anticancer drug. The formulation process is based on a low-energy nano-emulsification method and allows the generation of a structure composed of oil-based nanocarriers loaded with reverse micelles. Thanks to this, hydrophilic contents can be solubilised in the oily core of this kind of nano-emulsion along with lipophilic content. The results emphasise some original structure particularities due to the multistep formulation process, and the diffusion-based behaviour revealed for the DOX release profile that is shown to be intimately linked to the morphology of the particles.

1. Introduction

Doxorubicin hydrochloride (DOX) is commonly used in the treatment of many solid tumours, such as breast, lung, stomach or ovarian cancer and sarcoma. It inhibits cell growth by DNA intercalation, the generation of free radicals, interaction with cellular membranes and the inhibition of topoisomerase II [1]. Unfortunately, this anthracyclin has appeared to be highly toxic, by biodistribution to non-targeted tissues (heart mainly), causing severe side effects, limiting DOX dosage and harming to the patients comfort [2]. Therefore, in order to get round this critical point, research has focused on the development of new formulation strategies via DOX-encapsulated particulate drug delivery systems. CAELYX® provides an example of a commercial product, which is a DOX-containing liposomal PEGylated form available for the treatment of Aids-related Kaposi's sarcoma, advanced ovarian cancer and advanced breast cancer. More generally, drug encapsulation in colloidal systems offers many advantages, such as: (i) the protection of the drug against *in vivo* degradation, (ii) the reduction in potential toxic side effects occurring with the direct administration of solution-solubilising anticancer drugs, (iii) the increase in patient comfort by avoiding repetitive bolus injection or the use of perfusion pumps, and (iv) the achievement of more favourable drug pharmacokinetics [3]. In this way, many studies have been carried out with doxorubicin, giving rise to various DOX-containing nanoparticles, such as polymeric nanocarriers [4–8], inorganic magnetic nanoparticles where DOX is adsorbed onto their surface [9,10] or even solid lipid nanoparticles containing DOX as an ion-pair complex [11,12].

Eventually, since DOX is a hydrophilic and hydrosoluble molecule, the main challenge of these formulations remains that of entrapping DOX with a significant encapsulation rate and yield into such nanoparticulate systems that are themselves in suspension in aqueous solutions. More generally, this scope is included in the general field of encapsulating hydrophilic contents in nanoparticulate systems and has hence been the subject of much research. The main difficulties arise in controlling the hydrophilic, encapsulated molecule release, while also finding a good compromise between encapsulation efficiency, drug leakage induced by diffusion and/or by material degradation, the biocompatibility and biodegradation of particle components and the formulation processes (in the case of encapsulating fragile contents, adopting soft processes for limiting degradation is necessary).

In this context, the original purpose of this study concerns the formulation of lipid nanoparticulate systems, which combine all these latter points. These formulations are based on lipid nanoemulsions [13–16]. These nanoparticles, only formulated using biocompatible ingredients, are generated hrough a low-energy and solvent-free method (the phase inversion temperature method

* Corresponding author. University of Strasbourg, Faculty of Pharmacy, CNRS 7199, Laboratoire de Conception et Application de Molécules Bioactives, équipe de Pharmacie Biogalénique, 74 route du Rhin, F-67400 Illkirch, France.
E-mail address: nanton@unistra.fr (N. Anton).

0939-6411/$ - see front matter © 2011 Elsevier B.V. All rights reserved.
doi:10.1016/j.ejpb.2011.02.015

or PIT method) and present highly adjustable sizes [16] with a wide range of monodispersal size distribution. Accordingly, such a system is readily suitable for pharmaceutical applications. *in vitro*, and *in vivo* studies have disclosed for instance [17] an active role on the inhibition of the global multidrug resistance mechanism (MDR), hence increasing the inhibition of one ATP-efflux pump (P-glycoprotein) present in humans. This effect has been attributed to the PEG moiety of the non-ionic surfactant surrounding the nano-droplet surface [17]. In the case of anticancer drug administration, and a fortiori with DOX, this point is fundamental and reinforces the important role of PEGylated lipid nanocarriers.

The incorporation of hydrophilic or hydrosoluble contents in such lipid nano-objects is achieved by applying a simple idea that consists of incorporating a reverse micellar system to the nanocarrier lipid core since it solubilises hydrophilic molecule to be encapsulated [15,18]. Reverse micelles (RM) are multimolecular entities of surfactant in a non-polar medium. Reverse micellar system has been widely studied and reviewed [19–24] as it is a very simple and powerful system allowing the easy solubilisation of hydrophilic guests in oily phases. RM is a thermodynamically stable system; it forms spontaneously and is fully transparent. The most common application of RM is based on its use as a nano-reactor for nanoparticle formation or particular chemical syntheses [25]. A further potential of RM lies in their use as hydrophilic nano-reservoirs dispersed in a hydrophobic phase. Nevertheless, to date, except for a few examples [26,23], this option has not been extensively developed, mainly due to the continuous oily phase not being well adapted to the specifications inherent in the field of drug delivery and targeting. We have got round this problem in our study by subdividing this continuous oil phase for creating a stable nano-suspension, encapsulating the RM and producing different sizes. This was actually performed by taking advantage of the PIT process, which induces the spontaneous formation of nanocarriers without drastic treatment, and thus preventing the destruction of reverse micelles during emulsification.

In addition to these new features (*i.e.* the encapsulation of hydrophilic contents), these lipid nanocarriers still keep their ability to encapsulate hydrophobic molecules in the full, oily core of the nano-droplets; hence hydrophilic and hydrophobic molecules are encapsulated and stable in the same core. We recently pioneered this concept on another kind of nanoparticulate system based on aqueous-core nanocapsules [27], and we propose here a new and simple alternative with different technology. The great advantage of this technology, when two different drugs are entrapped in the same nanoparticle, lies in the fact that their simultaneous location is assured in the targeted site, and this can be highly interesting when their concomitant action is needed or is necessary for the treatment. As a result, efficiency should be increased and adverse effects reduced. This specific, synergic anticancer effect in multidrug resistant human breast cancer cells has been evidenced with the simultaneous co-encapsulation of DOX and mitomycin C in solid lipid/polymeric hybrid nanocapsules [28]. We chose to associate a lipophilic antineoplastic agent belonging to the taxoid family (which is docetaxel (DOCE)) to the DOX. This anticancer drug is used in association with DOX for the treatment of certain forms of breast cancer [29].

The different aspects related to the formulation and characterisation of these reverse micelle-loaded nanocarriers will be dealt with first. Then, the study will focus on the evaluation of encapsulation and release properties, of DOX alone and DOX associated with DOCE. In this work, our aim is not only to present this new technology, but also to show that it allows the encapsulation of two major anticancer drug contents with biocompatible formulations.

2. Materials and methods

2.1. Materials

The lipophilic Labrafac WL 1349® (caprylic-capric acid triglycerides; European Pharmacopeia, IVth, 2002) was provided by Gattefossé S.A. (Saint-Priest, France). Solutol HS 15® from BASF (Ludwigshafen, Germany), a mixture of free polyethylene glycol 660 and polyethylene glycol 660 hydroxystearate, European Pharmacopeia, IVth, 2002) was a kind gift from Laserson (Etampes, France). Water was obtained from a MilliQ filtration system (Millipore, Paris, France). Doxorubicin hydrochloride, docetaxel and Span 80® were purchased from Sigma (St Quentin Fallavier, France).

2.2. Drug solubilisation

In these low-energy nano-emulsification processes, the step of drug solubilisation is particularly important, and special care was dedicated to this.

Preliminary experiment showed that doxorubicin hydrochloride was absolutely not soluble in the medium chain triglycerides (Labrafac®) chosen here as oily phase in the absence of reverse micelles. Thus, DOX (2 mg) was solubilised in a reverse micelle suspension (5 mL) of Span 80® in Labrafac® (at a weight ratio of 1:5). The choice of Span 80® was due to its ability to self-organise in a non-polar medium and its biocompatibility [30]. The incubation was performed for 30 min, after which the DOX excess (*i.e.* non-solubilised remnant) was removed from the suspension by centrifugation. The precise amount of DOX loaded into the micelles was determined by making the difference after quantifying this excess, after solubilisation in DMSO, and by UV–visible spectroscopy (Uvikon 922®, Kontron Instruments, Milan) at 500 nm. The lipophilic DOCE was added to Labrafac® (1 wt.%) at the beginning of the formulation process and was entirely solubilised.

2.3. Nanocarrier formulation

The nanocarriers, like nano-emulsions, were prepared following the PIT method. This experimental procedure allows the preparation of small lipid nano-objects and presents many advantages, such as avoiding the use of organic solvent. This low-energy formulation process prevents the degradation of fragile drugs, is easy to handle, is rapid and inexpensive [15,31]. Briefly, Solutol® (39.3%), sodium chloride (1.8%), Labrafac® (17.2%) and water (41.7%) were mixed. This formulation was selected as a representative one based on our previous work [14,15]. The mixture was gently warmed until 90 °C under magnetic stirring at 500 rpm. Next, a slow cooling process was performed until 85 °C for which a given amount of reverse micelle-loaded oil was added to the mixture. Four different representative amounts of RM-loaded oil were selected: formulation A: 0.25 mL, formulation B: 1 mL, formulation C: 3 mL and formulation D: 5 mL. Afterwards, when the system, which was still cooling and homogenising, reached the PIT around 75 °C, a sudden dilution with room-temperature water was carried out (the dilution volume is six times the water volume in the mixture before dilution). The final oil contents are 20.4%, 28.6%, 44.1%, 54.0%, after the addition of 0.25, 1, 3, 5 mL of RM-loaded oil, respectively.

2.4. Size distribution and surface potential measurements

Nanocarrier size distribution (measured by dynamic light scattering, DLS) and zeta potential values were assessed using a Malvern NanoZS instrument (Malvern, Orsay, France). The

helium–neon laser, 4 mW, operates at 633 nm, with the scatter angle fixed at 173° and the temperature maintained at 25 °C. PDI is a measure of the broadness of a size distribution derived from the cumulants analysis of DLS data according to ISO 13321:1996; for a single Gaussian population with standard deviation, σ, and mean size, x_{PCS}, then $PDI = \sigma^2/x_{PCS}^2$ is the relative variance of the distribution. Measurements were performed three times for each point.

2.5. Transmission electron microscopy (TEM)

Observations were carried out by the SCIAM (Service Commun d'Imageries et d'Analyses Microscopiques) using a Jeol TEM 2011 (Croissy sur Seine, France) operating at 200 kV. Some suspensions were not stained before performing the measurements, and other ones were stained with a 4% osmium tetroxide solution, which specifically links with double bonds.

2.6. Freeze-drying

The behaviour of our lipid suspensions during the freeze-drying process was evaluated: 2 mL of the suspension was lyophilised in a LYOVAC GT2 (Steris, Germany) coupled to cryothermostat (UNISTAT 385®, Huber, Germany) system. Prior to freeze-drying, samples were frozen in liquid nitrogen.

2.7. Doxorubicin assay and encapsulation efficiency

Free DOX was removed from nanoparticles by steric exclusion chromatography: 100 µL of the suspension was deposited on a PD-10 desalting column and eluted with DPBS. Free and encapsulated DOX concentrations were determined by spectrofluorimetry (Fluoroscan, Ascent FL, Thermo Fisher Scientific, Cergy-Pontoise, France). The specific excitation and emission wavelengths of DOX were, respectively, 485 nm and 550 nm. Actually, the nanocarrier concentrations after the steric exclusion column are so low than the scattering effects due to the presence of the particles in the solution can be neglected. However, as the two media solubilising the drug are different (*i.e.* DPBS for free DOX, and reverse-micelle oil for DOX encapsulated in nanocarriers), two calibration curves had to be made. DOX encapsulation efficiency (EE) was given by the following Eq. (1).

$$EE(\%) = \frac{\text{Encapsulated DOX amount} \times 100}{\text{DOX total amount}} \quad (1)$$

2.8. Docetaxel assay and encapsulation efficiency

The encapsulated docetaxel was quantified by a HPLC method. Firstly, filtration (0.2 µm Minisart filter cellulose acetate, Sartorius, France) was performed on the nanoparticle suspension to remove free docetaxel. The nanoparticles were then dissolved in methanol (1/12) and finally filtered once before HPLC measurement.

Chromatography was performed using a Waters Alliance® 2690 system (Waters SA, Saint Quentin en Yvelynes, France) with a Hichrom (Hichrom Ltd., Berkshire, UK) RPB 250 mm × 4.6 mm, 5 µm particles column, coupled to a pre-column (Hichrom Ltd., Berkshire, UK). The detection wavelength was 230 nm. The mobile phase was composed of a gradient of water (solvent A) and acetonitrile (solvent B), kept as T/%B : 0/35, 15/65, 25/75, 30/95, 35/100, 39/100 and 40/35, with a post-run time of 10 min, at a flow rate of 1 mL min^{-1}. The injection volume was 10 µL. The encapsulation efficiency (%) was calculated comparing the total DOCE used in the formulation with the encapsulated amount.

2.9. In vitro release studies

Release experiments of DOX were performed by incubating 4 mL of formulation with the RM-loaded content corresponding to the proportions B and C, in dialysis tubing (diameter 16 mm, MWCO 7000 Da, Medicell International, London, UK) in 70 mL of Dulbecco's Phosphate Buffer Saline (DPBS, pH = 7.4, C = 0.1 M) at 37 °C and gently stirred magnetically. At predetermined time points, the dialysate was sampled (aliquots of 1 mL) and replaced by the same volume of fresh medium to assure sink conditions (even if the volume of the release medium used was enough to dissolve at least four times the quantity of drug present in nanoparticles [32]). The semi-empirical power law presented in Eq. (2) was used to fit the experimental data [6,33,34].

$$\frac{M_t}{M_\infty} = \frac{M_b}{M_\infty} + kt^n \quad (2)$$

M_t, M_∞ are the amount of drug release at respectively time t and infinite time, M_b corresponding to the amount of burst-release drug, k is a constant incorporating structural and geometric characteristics of the device and n is the release exponent, indicative of the mechanism of drug release. According to such a model proposed by Siepmann and Peppas [33,34,6], and in our case of spherical geometry, the values of n range from 0.43 to 0.85 corresponding, respectively, to a Fickian diffusion and a case-II transport [35,36].

3. Results

3.1. Nanoparticle characterisation

The reverse micelle-loaded nanocarriers basically constitute a novel drug delivery nanoparticulate system. The first stage of this study is a global physicochemical characterisation of the nanoparticles formed, *i.e.* size distribution and surface potential. The influence of the blank RM-loaded oil added to the formulation on the size distribution and zeta potential is shown in Fig. 1. A net trend arises showing highly linear behaviour of the size increase and zeta potential decrease. This result appears coherent with our previous study [37,14] giving a size rise with the increase in the whole initial oil amount. In addition, the PDI values (labels on the figure) indicate narrow size distributions. As far as the surface potential is concerned, it appears globally negative, but with values varying

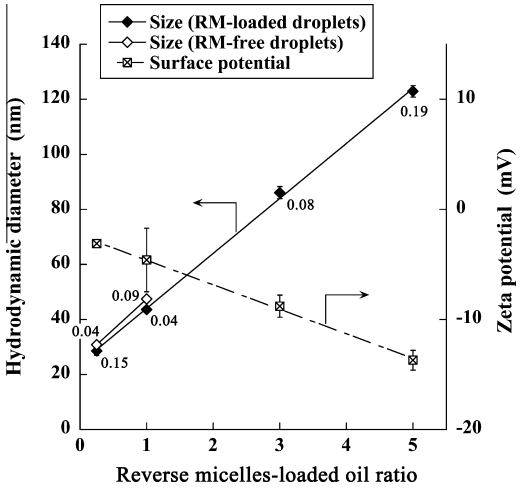

Fig. 1. Characterisation of blank reverse micelles-containing nanocarriers. Size distribution by DLS: influence of the RM-loaded oil added on the size distribution, filled symbols, the labels are polydispersity indexes. Surface potential measurements by zetametry, open symbols.

from (−3.1 ± 0.2) to (−13.7 ± 0.9) mV which still remain weak (due to the non-ionic character of the content). Likewise, we studied here the impact of the presence of the RM on the nano-emulsions formulation, by performing the process similarly, adding the same oil volumes but without reverse micelles. The results are included in Fig. 1 (open symbols). It appears that the formulation was only possible for the smaller oil volumes added (0.25 mL and 1 mL), whereas for the higher (3 mL and 5 mL) it gives only rise to heterogeneous and unstable systems. It means that the presence of surfactant in oil plays a significant role at the water/oil interface, enabling the formation of nano-droplets. Concerning the size obtained for 0.25 mL and 1 mL without reverse micelles, only an increase in a few nanometres is observed. This could come from the fact that a minimal amount of surfactant is needed in the PIT process to allow the nano-scaled droplets formation. For the lower oil volumes added, the initial surfactant amount is sufficient, but for the higher oil volumes, the amphiphiles are missing with the addition of RM-free oil, whereas their are brought with the reverse micelles.

It would be important to note here that micelles are thermodynamically systems, and the amphiphiles molecules (Span 80®) taking part of these self-associated systems are actually in equilibrium between associated and free configuration (such an equilibrium being strongly shifted towards the micelle formation). That also means that the micellisation process is a spontaneous process, and the micelles form rapidly and spontaneously when the concentration is higher than the CMC. It is actually the case here since the surfactant concentration in oil is around 20 wt.%. Besides, the whole comprehensive study concerning the impact of the formulation parameters, like the RM concentration in oil, on the EE and nano-emulsion properties, has been already done and published elsewhere with a model hydrophilic molecule (fluorescein sodium salt). Actually, Fig. 5 in Ref. [15] shows the encapsulation yields and fluorescein concentration in the nano-emulsion droplets, as a function of the fluorescein concentration in oil (as a function of the micelles concentration), and we showed any influence on the encapsulation yields, along with a linear increase in the concentration in droplets. This result means that increasing the micelles concentration does not impact (i) on the formulation process, *i.e.* on the nano-emulsion properties (droplet size, morphology), as well as (ii) on their ability to maintain the hydrophilic molecules in oil, keeping constant the encapsulation yields. It is also to be noted that the formulation D (with RM-loaded oil volume = 5 mL) destabilises quite quickly, *i.e.* within a few hours, which is also confirmed by a PDI slightly higher than all the other samples.

Fig. 2 presents TEM micrographs of these micelle-loaded nanoparticles contrasted with a specific marker for double bonds, osmium tetroxide (Fig. 2a and b), and without any staining (Fig. 2c and d). The TEM experiments were performed on each samples and formulations, and we propose in Fig. 2 the representative case of RM-loaded oil volume = 3 mL. The first observation corroborates the size range of the nanoparticles with the DLS measurements, centred around 90 nm for this example (with RM-loaded oil volume = 3 mL). Then, Fig. 2a and b revealed a quite spherical and homogeneous structure, well contrasted by osmium tetroxide. This contrasting agent is generally used in TEM techniques as a lipid-staining agent due to its ability to specifically fix itself on the lipid insaturations. However, since Labrafac CC® and Solutol HS15® fatty chains are fully saturated, whereas Span 80® is insaturated, the micrograph contrasted area should indicate the specific Span 80® location and thus is a reverse micelle marker. Under these considerations, and bearing in mind that TEM images are projections of the objects on one plane, the repartition of reverse micelles appears globally to provide a homogeneous spread among the different particles in Fig. 2a and also with the same particles in Fig. 2b.

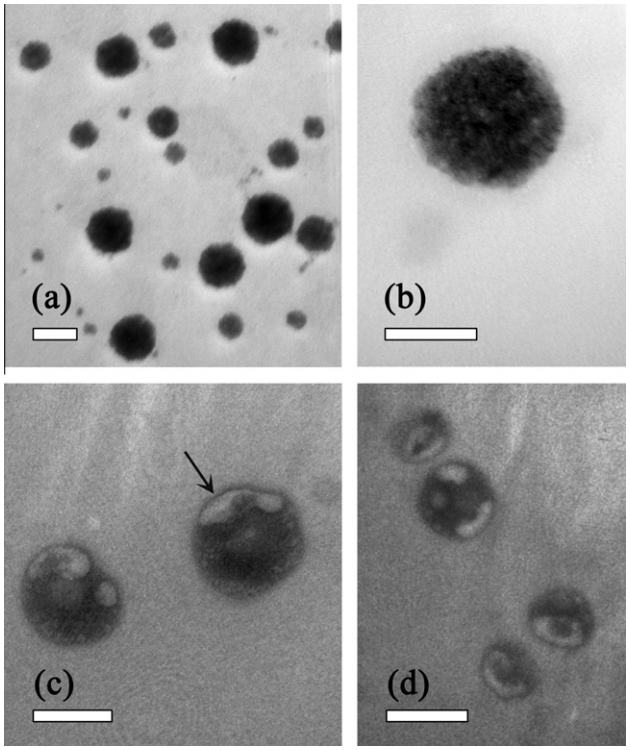

Fig. 2. TEM micrographs of the RM-loaded nanocarriers (added oil volume = 3 mL), (a) and (b) contrasted with osmium tetroxide; (c) and (d) without staining. The scale bars are 100 nm.

However, the samples observed without staining agent (Fig. 2c and d), surprisingly let light out a demixtion phenomenon on the same particle: one part appears almost non-contrasted, and the remaining major other part is significantly more contrasted. Without the use of staining agent, the contrast on such micrographs was software enhanced and thus, allowed these details to be revealed.

3.2. Freeze-drying nanoparticles

One strong particularity of these nanocarriers is their ability to bear a freeze-drying process without cryoprotectant, and without important change in their sizes and surface potentials. This is generally not the case with lipid nano-emulsions or lipid nanocapsules (LNC) systems [38] and simply means that the release of encapsulated drugs will be suspended until the reconstitution of the product. After freeze-drying is complete, the nanoparticle resuspension in water is performed in one minute under a gentle magnetic agitation. The results are summarised in Table 1, comparing droplet size and zeta potential before and after freeze-drying.

The first important point to note is the conservation of the global monodispersity of the samples throughout the freeze-drying process. The slight PDI increase, observed for the formulations B and C, can be however attributed to the process which is not totally harmless. This result means that the homogeneity of the dispersion and the nano-droplet structure are not affected by the process and make the use of freeze-drying a possible way for conservating for the product for packaging.

3.3. Drug nano-encapsulation

3.3.1. DOX encapsulation in nanocarriers

This section concerns the main objective of this study, that is, the encapsulation and release of a hydrophilic anticancer product into lipid nanocarriers. As previously described, DOX is solubilised

Table 1
Impact of the freeze-drying process on the nanocarrier hydrodynamic diameter (d), polydispersity index (PDI), and surface potential (zeta potential, ζ).

Formulations	Before freeze-drying			After freeze-drying		
	d (nm)	PDI	ζ pot. (mV)	*d* (nm)	PDI	ζ pot. (mV)
A	28.9 ± 1.6	0.15 ± 0.04	−3.1 ± 0.2	28.0 ± 0.2	0.14 ± 0.01	−3.4 ± 0.3
B	43.6 ± 0.7	0.04 ± 0.01	−4.6 ± 2.9	49.0 ± 5.4	0.16 ± 0.02	−9.8 ± 0.6
C	86.1 ± 2.2	0.08 ± 0.02	−8.8 ± 1.0	108.2 ± 2.0	0.16	−19 ± 0.5

in a suspension Span 80® reverse micelles. As a thermodynamically stable system, the formed micelles are definitively stable once formed and loaded. However, in the presence of the aqueous phase (*i.e.* aqueous parts of the microemulsion systems in the phase inversion zone), this equilibrium is upset, which results in a transfer of the ingredients loaded into the micelles in oil towards this polar phase, across the oil/water interface. Also, the presence of an oil/water interface disturbs the equilibrium, inducing a migration of the Span 80® towards this interface and a destruction of the molecular associations. These two latter points are precisely the purpose of studying and controlling DOX encapsulation and release.

The DOX concentration incorporated in the RM system was obtained at (0.152 ± 0.012) mg mL^{-1}, corresponding to an incorporation yield of around 40%. Once DOX solubilisation in micelles is achieved, the suspensions are stable and no recrystallisation occurred for months.

The encapsulation efficiency (EE) of DOX is reported in Fig. 3 in function of the representative RM-loaded oil volume = 0.25, 1 and 3 mL and compared to the increase in size (the values of the size come from Fig. 1, showing a linear increase with the added oil volume). The encapsulation efficiency appears to fluctuate between (37 ± 6)% and (68 ± 4)% and is not linked to the RM-loaded oil added, droplet size, the whole-oil volume or even droplet-specific surface. This result means that the encapsulated and free parts of DOX do not depend on the RM-loaded oil volume and on size.

3.3.2. In vitro DOX release

Fig. 4 presents the *in vitro* release kinetics of the DOX, loaded in formulations B (filled squares) and C (open circles). According to Eq. (2), we ventured the hypothesis that only a Fickian diffusion governed the drug release, *i.e.* the value of the parameter *n* was assumed equal to 0.43. In addition, as described in the literature [6], release profiles at 37 °C are assumed to present a burst release, giving rise to consider in our case a value of $\frac{M_b}{M_\infty} = 0.03$. The experimental results actually confirmed quite well these assumption, as it is illustrated in Fig. 4 (R = 0.982 and 0.962, respectively, for the 44 nm and 95 nm particles).

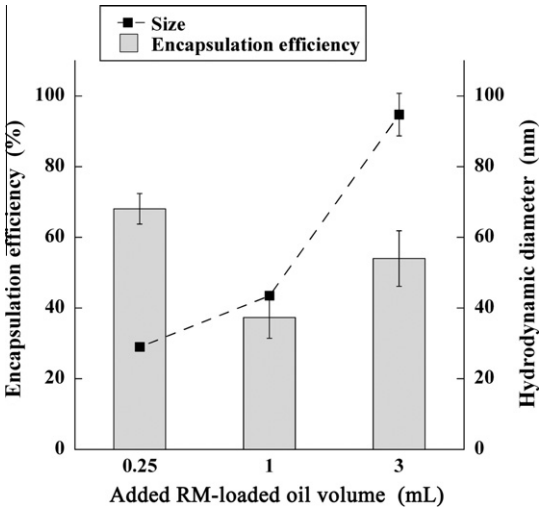

Fig. 3. DOX-loaded nanocarriers: encapsulation efficiency and size, for three representative oil volumes = 0:25, 1 and 3 mL.

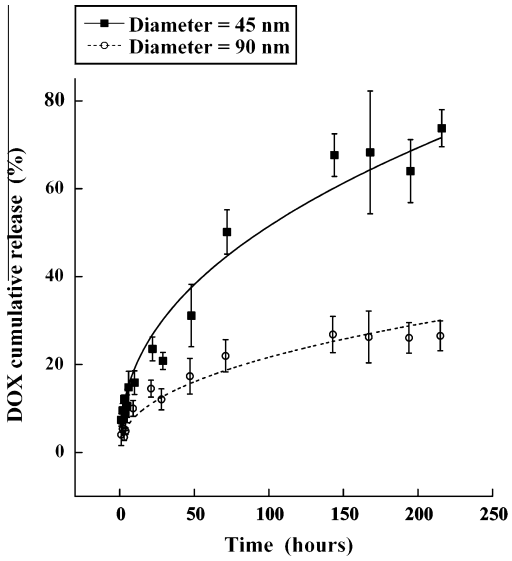

Fig. 4. DOX release kinetics at 37 °C in PBS, for two formulations with added RM-loaded oil volume = 1 mL (filled square, diameter = 44 nm) and 3 mL (open circles, diameter = 95 nm). Fit to the semi-empirical power law (Eq. (2), see details in the text).

3.4. Doxorubicin and docetaxel co-encapsulation

In this section, we show the potential of simultaneously encapsulating hydrophilic (DOX) and lipophilic (DOCE) drugs in nanoparticles. This drug association is even more interesting in that it is routinely performed in the treatment of certain breast tumours. DOX is entrapped in a reverse micellar system, whereas DOCE is solubilised in the same nanoparticle, in the oily core. The results are summarised in Table 2, comparing two formulations B (RM-loaded oil volume = 1 mL), one only loaded with DOX and the

Table 2
Simultaneous encapsulation of hydrophilic and lipophilic anticancer drugs (DOX and DOCE) in the same nano-droplets. B^{DOX} and $B^{DOX+DOCE}$, respectively, refer to nanocarrier only loaded with DOX and nanocarrier loaded with both DOX and DOCE. Nanocarrier properties are summarised with their hydrodynamic diameter (d), polydispersity index (PDI), and surface potential (zeta potential, ζ), and with the corresponding anticancer encapsulation efficiency (EE).

Formulations	Nanocarriers properties			Anticancer EE (%)	
	d (nm)	PDI	ζ pot. (mV)	DOX	DOCE
B^{DOX}	43.5 ± 0.7	0.04 ± 0.01	−5.9 ± 0.6	37.3 ± 5.9	-
$B^{DOX+DOCE}$	42.7 ± 0.7	0.05 ± 0.01	−2.6 ± 0.5	29.6 ± 0.3	103.4 ± 2.6

other with DOX and DOCE. These results clearly show the potential of this new technology for the co-encapsulation of different contents with different partitioning coefficients. Nanoparticle morphology and size distribution remain unchanged with or without the presence of drugs, and the surface potentials undergo a weak decrease.

4. Discussion

The physicochemical characterisation provides basic results on both the RM-loaded oil incorporation step in the nanocarrier generation process and the formed nanocarrier. Their narrow size distribution actually means that the RM-loaded oil added in the formulation is homogeneously shared out with the initial oil before water dilution, and thus in the resulting lipid nanoparticles. On the other hand, the linear growth of the particle diameter (R^2 = 0.998) shows that the nanocarrier formation is fully related to the formulation parameters as it is in the case of the conventional PIT process or spontaneous emulsification [16]. This highlights the fact that all these formulating processes are governed by one unique mechanism. The linear decrease in the zeta potential values follows an increase in the curvature of the oil/water interface as well as the increase in the Span 80® concentration in oil. Consequently, it leads to modifications of the interface composition and PEG chain organisation. Owing to their ability to change their partitioning coefficient with the temperature, the hydrophilic non-ionic surfactants, Solutol HS15®, constitute the main actors of the low-energy nano-emulsification process [16,39,40], probably covers the majority of the water oil interface. On the other hand, the main role of the lipophilic surfactant (Span 80®) is the formation of reverse micelles for solubilising the DOX.

In addition, the TEM results not only corroborate the size ranges disclosed by dynamic light scattering, but also highlight one original particle morphology very specific to this formulation process. This "two-domains" morphology can be explained by the reduced miscibility of the two lipid phases (with or without reverse micelles) which could potentially be due to various reasons, such as their difference in viscosity, composition or the short homogenisation time allowed by the process before their break-up into dispersed droplets. Moreover, since the value of the added RM-loaded oil volume was fixed at 3 mL, we suggest that the contrasted part could presumably be the RM-loaded oil part, contrasted thanks to the presence of surfactant molecules denser than oleic ones. This point is endorsed by the contrast arising on the surrounding frontier of the nanoparticles (see the arrow in Fig. 2c), concentrated in surfactant molecules. It is to be noted here, the existence of such a structure can highlight the question of the optimisation of the process, *i.e.* in the case for which the RM-free oil could be fully substituted by the RM-loaded oil. Actually, it is not possible, since (data not shown) if the non-loaded oil is substituted for a RM-loaded one at the beginning of the process, the DOX leakage (towards the water phase) during all the steps of the process is dramatically increased, and thus the final encapsulation efficiency dramatically decreased, near to zero.

At this point, a probable structure of this complex nanoparticulate system can be provided through the schematic representation presented in Fig. 5. The oil nano-droplets, composed of reverse micelles and micelle-free non-mixed zones, are surrounded by a mixed surfactant layer. Hydrophilic non-ionic surfactant, Solutol HS15®, as the main actor in the low-energy nano-emulsification process [16], probably covers the majority of the water/oil interface, whereas the lipophilic, other non-ionic Span 80®, temporarily occupies the layer. The PEG moiety of Solutol HS15® creates a hydrophilic shell, which is known to decrease the particle uptake rate itself by the reticulo-endothelial system (RES). It is fundamental to note here that such a structure is a metastable structure, potentially fragile but stable, and the only reason which allows its establishment is that the formulation follows a low-energy process [13]. In this way, the micellar structure can be conserved during the oil break-up forming nano-droplets. Likewise, the possibility to freeze-dry such nanocarriers, besides constituting yet a significant results, also means that the surfactant layer stabilising the water/oil interface presents an interfacial structure strong, flexible and stable enough to protect the particles against coalescence. This could explain the prevention of micelle leakage when the particles are in suspension.

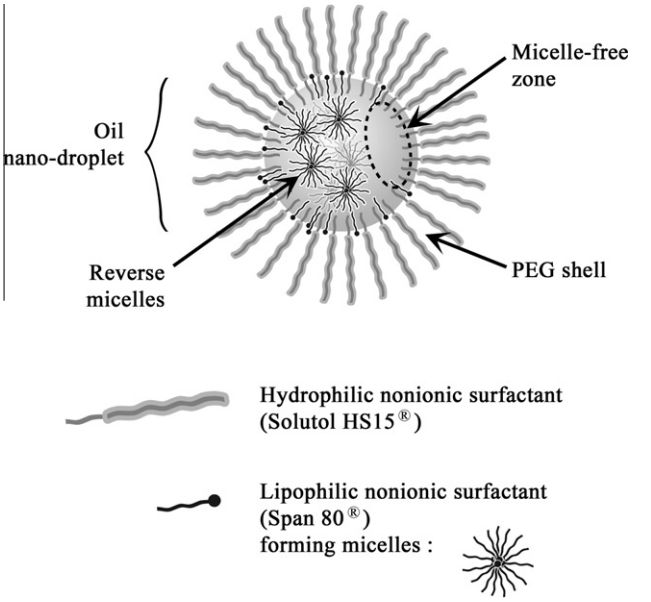

Fig. 5. Schematic representation of the reverse micelle-loaded nanocarriers (see details in the text).

As well, beyond the DOX encapsulation itself into these nanocarriers which constitutes the main results of this study, this also suggests that the particle formulation mechanism, explained by the very fast transfer of the hydrophilic surfactant towards the aqueous phase [16], does sweep along a similar amount of hydrophilic content, whatever the proportions of the surfactants. The RM system is stable enough to maintain encapsulated more than half of the encapsulated anticancer drug, allowing its controlled release. As a final remark, the surface potential measurements (data not shown) do not present a significant difference compared to the results with blank nanocarriers reported in Fig. 1, which can confirm DOX entrapment in the nanoparticles' oily core. Protection of the anticancer drug against inconvenient action or drug degradation is thereby assured. Similar encapsulation and morphological properties are obtained after the freeze-drying process.

Next, by definition, regarding both the encapsulation efficiency which does not reach 100%, and the sustained release obtained, it is clear that a drug leakage occurs during the formulation step into the PIT. Owing to the significant Span 80® concentration in oil (20 wt.%), the slight dilution during the described process can absolutely not decrease the concentration below the Span 80® CMC, which is around 0.007 mg/mL [41]. As a result, the potential Span dilution in oil (even if the two oil domains observed in TEM are mixed) cannot result in the micelles breaking-up and in the DOX release. Actually, the DOX leakage observed during the formulation step seems likely due to the breaking-up of micelles at the vicinity of the water/oil interface, and thus giving rise to the transfer of a given amount of DOX towards the aqueous phase. This prematurely released DOX is removed from the nano-emulsion

suspensions through the PD-10 column. This separation is performed within a few minutes and has been considered negligible compared to the whole release kinetics of DOX (around 9 days).

The release mechanisms are disclosed in Fig. 4 as controlled by the Fickian diffusion. It actually appears coherent with drug encapsulation solubilised in free reverse micelles in oil, for which the leakage is performed either by diffusion through the oil barrier or by micelle transport towards the oil/water interface. By extrapolating the diffusion-controlled Higuchi model [34,42], we will also assume that in our case, described by the power law Eq. (2), the values of the parameter $k^{\frac{1}{0.43}}$ are linearly correlated to the diffusion coefficient D of the released content. We finally found $\left(\frac{k^C}{k^B}\right)^{\frac{1}{0.43}} \sim \frac{D^C}{D^B}$ about 7.512, with k^B and k^C, D^B and D^C, the constants and the diffusion coefficients for the formulation B (44 nm particles) and C (95 nm particles), respectively. This difference confirmed the one expected for two systems having different specific surfaces, that is to say an interfacial areas ratio calculated at ~10.865 taking into account the difference in (RM-containing) oil volumes added during the processes. Even if these values show the same order of magnitude, the difference observed between the formulations B and C may have originated for various reasons, such as for instance the difference in the specific surfaces or the difference in surfactant interfacial concentration acting as a barrier against the drug leakage.

Besides lowering the potential adverse effects of the administration of free drugs, the release profile given by these nanocarriers is well controlled and predictable. This could be a considerable advantage compared to commercially available liposome-based formulations (for which the break-up of the liposome membrane is not controlled) in the case of therapeutic strategies based on active or passive targeting.

The docetaxel physicochemical properties do not allow observing any release in water; accordingly, the following-up of its release has not been carried out. Moreover, the main interest of DOCE entrapment in lipid nanocarriers is the formulation of a "solubilised form" of the drug in an aqueous phase, facilitating its administration. In addition, the absence of DOCE release from nanocarriers does not appear as a limit to its efficacy, and the nanoparticulate suspension presents an enhanced penetration into the tissues and cells (potentially combined with targeting strategies). Finally, the neutral role of the encapsulated molecules on the droplet formation mechanism is shown with the last example of concomitant DOX and DOCE encapsulation, presenting any significant change on the particle size. On the other hand, the concomitant presence of the two drugs in the same droplets appears to ensue into a slight drop of the DOX encapsulation yields. This could be due to different reasons, such as a reduced solubility of DOX in the solubilising medium, or that its nature is changed by the presence of DOCE. The two encapsulated drugs have very different physicochemical properties, and the formulations were actually adapted to these properties. The very low solubility of the docetaxel in water, notably, makes expect a negligible release of DOCE, that is to say, the potential adaptation of the administration of these nano-systems to the treatment of tumours could only be tailored to the release behaviour of DOX, as well as, of course, to the loading rates of both the encapsulated drugs.

5. Conclusion

This study was initiated with the aim of formulating a hydrophilic nanocarrier for protecting very reactive species like anticancer drugs. In this way, a new technological process was developed proposing new multifunctional lipid nano-systems allowing the simultaneous encapsulation of hydrophilic and lipophilic drugs. The drug nanocarriers are formulated through an innovative low-energy and solvent-free process, and only use pharmaceutically acceptable compounds. The nanoparticles were thoroughly characterised and revealed the presence of a multiscale reverse micelle-in-oil-in-water structure compatible with the encapsulation and the sustained release of drugs. A hydrophilic model anticancer drug, DOX, is solubilised in micelles, whereas a lipophilic one, DOCE, is naturally dissolved in the oily core of the nanocarriers. The size distribution and polydispersity were shown as being highly controllable, and likewise linked to the diffusion-release kinetics. Finally, owing to the different properties of these nanocarriers in terms of encapsulation efficiency and release profile, they appear as an interesting alternative to the existing liposome-based, commercially available products for anticancer drug administration.

Acknowledgments

The authors thank the SCIAM (Service Commun d'Imageries et d'Analyses Microscopiques) of Angers (France) for the TEM analysis.

References

[1] A. f. d. e. d. c. t. AFECT (Ed.), Médicaments antitumoraux et perspectives dans le traitement des cancers, vol. 6, Tech & Doc, Paris, pp. 364–411.
[2] A. Allen, The cardiotoxicity of chemotherapeutic drugs, Semin. Oncol. 19 (1992) 529–542.
[3] R. Gref, A. Domb, P. Quellec, T. Blunk, R. Muller, J. Verbavatz, R. Langer, The controlled intravenous delivery of drugs using peg-coated sterically stabilized nanospheres, Adv. Drug Deliv. Rev. 16 (1995) 215–233.
[4] M. Chavanpatil, A. Khdair, J. Panyam, Surfactant-polymer nanoparticles: a novel platform for sustained and enhanced cellular delivery of water-soluble molecules, Pharm. Res. 24 (2007) 803–810.
[5] C. Liu, W. Fan, X. Chen, C. Liu, X. Meng, J. Park, Self-assembled nanoparticles based on linoleic-acid modified carboxymethyl-chitosan as carrier of adriamycin (adr), Curr. Appl. Phys. 7 (2007) 125–129.
[6] D. Missirlis, R. Kawamura, N. Tirelli, J.A. Hubbell, Doxorubicin encapsulation and diffusional release from stable, polymeric, hydrogel nanoparticles, Eur. J. Pharm. Sci. 29 (2006) 120–129.
[7] S. Yang, H. Ge, Y. Hu, X. Jiang, C. Yang, Doxorubucin-loaded poly(butylcyanoacrylate) nanoparticles produced by emulsifier-free emulsion polymerization, J. Appl. Polym. Sci. 78 (1999) 517–526.
[8] L. Qiu, R. Wang, C. Zheng, Y. Jin, J.Q. Le, Beta-cyclodextrin-centered star-shaped amphiphilic polymers for doxorubicin delivery, Nanomedicine 5 (2010) 193–208.
[9] M. Brzozowska, P. Krysinski, Synthesis and functionalization of magnetic nanoparticles with covalently bound electroactive compound doxorubicin, Electrochim. Acta 54 (2009) 5065–5070.
[10] S. Guo, D. Li, L. Zhang, J. Li, E. Wang, Monodisperse mesoporous superparamagnetic single-crystal magnetite nanoparticles for drug delivery, Biomaterials 30 (2009) 1881–1889.
[11] A. Fundaro, R. Cavalli, A. Bargoni, D. Vighetto, G. Zara, M. Gasco, Non-stealth and stealth solid lipid nanoparticles (sln) carrying doxorubicin: pharmacokinetics and tissue distribution after i.v. administration to rats, Pharmacol. Res. 42 (2000) 337–343.
[12] H. Wong, A. Rauth, R. Bendayan, J. Manias, M. Ramaswamy, Z. Liu, S. Erhan, X. Wu, A new polymer-lipid hybrid nanoparticle system increases cytotoxicity of doxorubicin against multidrug-resistant human breast cancer cells, Pharm. Res. 23 (2006) 1574–1585.
[13] N. Anton, J.-P. Benoit, P. Saulnier, Design and production of nanoparticles formulated from nano-emulsion templates – a review, J. Control. Release 128 (3) (2008) 185–199.
[14] N. Anton, P. Gayet, J. Benoit, P. Saulnier, Nano-emulsions and nanocapsules by the pit method: an investigation on the role of the temperature cycling on the emulsion phase inversion, Int. J. Pharm. 344 (2007) 44–52.
[15] N. Anton, H. Mojzisova, E. Porcher, P. Saulnier, J. Benoit, Reverse micelles-loaded lipid nano-emulsions: a new technology for the nano-encapsulation of hydrophilic materials, Int. J. Pharm. 398 (2010) 204–209.
[16] N. Anton, T. Vandamme, The universality of low-energy nano-emulsification, Int. J. Pharm. 377 (2009) 142–147.
[17] E. Garcion, A. Lamprecht, B. Heurtault, A. Paillard, A. Aubert-Pouessel, B. Denizot, P. Menei, J. Benoit, A new generation of anticancer, drug-loaded, colloidal vectors reverses multidrug resistance in glioma and reduces tumor progression in rats, Mol. Cancer Ther. 5 (2006) 1710–1722.
[18] P. Saulnier, J. Benoit, N. Anton, Nanocapsules with liquid lipidic core loaded with water-soluble or water-dispersible ingredient(s), 2008.
[19] M.-C. Jones, P. Tewari, C. Blei, K. Hales, D. Pochan, J.-C. Leroux, Self-assembled nanocages for hydrophilic guest molecules, J. Am. Chem. Soc. 128 (2006) 14599–14605.

[20] M. Jones, J. Leroux, Reverse micelles from amphiphilic branched polymers, Soft Matter 6 (2010) 5850–5859.
[21] G. Gaucher, P. Satturwar, M. Jones, A. Furtos, J. Leroux, Polymeric micelles for oral drug delivery, Eur. J. Pharm. Biopharm. 76 (2010) 147–158.
[22] H. Kim, B. Lee, H. Sah, Reverse micelle-based microencapsulation of oxytetracycline hydrochloride into poly-D,L-lactide-co-glycolide microspheres, Drug Deliv. 14 (2007) 95–99.
[23] J. Liu, T. Gong, C. Wang, Z. Zhong, Z. Zhang, Solid lipid nanoparticles loaded with insulin by sodium cholate-phosphatidylcholine-based mixed micelles: preparation and characterization, Int. J. Pharm. 340 (2007) 153–162.
[24] A. Miller, A. Bershteyn, W. Tan, P. Hammond, R. Cohen, D. Irvine, Block copolymer micelles as nanocontainers for controlled release of proteins from biocompatible oil phases, Biomacromolecules 10 (2009) 732–741.
[25] V. Uskokovic, M. Drofenik, Reverse micelles: inert nano-reactors or physico-chemically active guides of the capped reactions, Adv. Colloid Interface Sci. 133 (2007) 23–34.
[26] F. Cui, K. Shi, L. Zhang, A. Tao, Y. Kawashima, Biodegradable nanoparticles loaded with insulin-phospholipid complex for oral delivery: preparation, in vitro characterization and in vivo evaluation, J. Control. Release 114 (2006) 242–250.
[27] N. Anton, P. Saulnier, C. Gaillard, E. Porcher, S. Vrignaud, J. Benoit, Aqueous-core lipid nanocapsules for encapsulating fragile hydrophilic and/or lipophilic molecules, Langmuir 25 (2009) 11413–11419.
[28] A. Shuhendler, R. Cheung, J. Manias, A. Connor, A. Rauth, X. Wu, A novel doxorubicin-mitomycin c co-encapsulated nanoparticle formulation exhibits anti-cancer synergy in multidrug resistant human breast cancer cells, Breast Cancer Res. Treat. 119 (2009) 255–269.
[29] Cytotoxiques: utilisation pratique, Centre National Hospitalier d'Information sur le Médicament, 1998.
[30] R. Strickley, Solubilizing excipients in oral and injectable formulations, Pharm. Res. 21 (2004) 201–230.
[31] B. Heurtault, P. Saulnier, B. Pech, J. Proust, J. Benoit, A novel phase inversion-based process for the preparation of lipid nanocarriers, Pharm. Res. 19 (2002) 875–880.
[32] M. Chavanpatil, A. Khdair, Y. Patil, H. Handa, G. Mao, J. Panyam, Polymer-surfactant nanoparticles for sustained release of water-soluble drugs, J. Pharm. Sci. 96 (2007) 3379–3389.
[33] N. Peppas, Analysis of fickian and non-fickian drug release from polymers, Pharm. Acta Helv. 60 (1985) 110–111.
[34] J. Siepmann, N. Peppas, Modeling of drug release from delivery systems based on hydroxypropyl methylcellulose (hpmc), Adv. Drug Deliv. Rev. 48 (2001) 139–157.
[35] T. Wang, T. Kwei, H. Frisch, Diffusion in glassy polymers, iii, J. Polym. Sci. 7 (1968) 2019–2028.
[36] G. Park, Synthetic Membranes: Science, Engineering and Applications, Reidel, D. Publishing Company, Dordrecht, pp. 57–108.
[37] B. Heurtault, P. Saulnier, B. Pech, M. Venier-Julienne, J. Proust, R. Phan-Tan-Luu, J. Benoit, The influence of lipid nanocapsule composition on their size distribution, Eur. J. Pharm. Sci. 18 (2003) 55–61.
[38] C. Dulieu, D. Bazile, Influence of lipid nanocapsules composition on their aptness to freeze-drying, Pharm. Res. 22 (2005) 285–292.
[39] N. Anton, P. Saulnier, A. Beduneau, J. Benoit, Salting-out effect induced by temperature cycling on a water/nonionic surfactant/oil system, J. Phys. Chem. B 111 (2007) 3651–3657.
[40] N. Anton, J. Benoit, P. Saulnier, Particular conductive behaviors of emulsions phase inverting, J. Drug Deliv. Sci. Technol. 18 (2008) 95–99.
[41] L. Peltonen, J. Yliruusi, Surface pressure, hysteresis, interfacial tension, and cmc of four sorbitan monoesters at water–air, water–hexane, and hexane–air interfaces, J. Colloid Interface Sci. 227 (2000) 1–6.
[42] P. Soo, L. Luo, B. Maysinger, A. Eisenberg, Incorporation and release of hydrophobic probes in biocompatible polycaprolactone-block-poly(ethylene oxide) micelles: implications for drug, Langmuir 18 (2002) 9996–10004.